Quantification of spine surgery　Finite element method for nerve root decompression spine minimally invasive endoscopic surgery

Thesis

Quantification of spine surgery

Finite element method for nerve root decompression spine minimally invasive endoscopic surgery

Yoshihiro Kitahama

Cooperative Major of Medical Photonics

Hamamatsu University School of Medicine

Faculty of Engineering, Shizuoka University

Hamamatsu, Japan

Abstract

Introduction: Diagnosis is the key to improving spinal surgical outcomes. Full endoscopic spinal surgery (FESS) can create new indications when the diagnosis of radiculopathy is improved. We assessed the finite element method (FEM) to visualize and digitize lesions not detected by conventional diagnostic imaging.

Methods: The lumbar patient was a 67-year-old woman with a history of rheumatoid arthritis, and with osteoporosis and pulmonary fibrosis. She had left L3 radiculopathy due to an L3 vertebral fracture. The cervical patient was a 61-year-old woman with left C6 radiculopathy due to C5-6 disc herniation. We performed full endoscopic foraminotomy on the patient's request. Based on CT DICOM data of 0.5-mm slices preoperatively and postoperatively, 3D imaging data were reproduced by Mechanical Finder®, and kinetic simulation of FEM was performed.

Results: Postoperatively, their radiculopathy disappeared, improving their activities of daily living, and enabling them to walk and work. The total contact area and maximum contact pressure of the nerve tissue decreased to 30%-80% and 33%-67%, respectively, postoperatively.

Conclusions: FEM can be a new method for perioperative evaluation and simulation to visualize and digitize the conditions of the lesion causing radiculopathy. FEM that can overcome both time and economic constraints in routine clinical practice is needed.

Keywords: finite element method, foraminotomy, full endoscopic spine surgery

1. Introduction

The finite element method(FEM) has been utilized to analyze the developmental mechanism of the fracture of bone components which are hard materials, and to judge the effects of fixation[1-10]. Additionally, preoperative simulation using a 3D printed model is now covered by the National Health insurance[11-12]. Utilization of 3D reconstituted images for navigation based on CT DICOM data has also been progressing in the spinal surgery field[13]. However, no kinetic imaging diagnosis method capable of sufficiently expressing the effects of less invasive nerve root decompression such as full endoscopic spinal surgery(FESS) has been developed.

Visualization and quantification of pain are important unsolved issues in the medical field[20-22]. If these are possible, pain can be accurately diagnosed, and treatment outcomes and activities of daily living can be improved, which may reduce medical expenses. Presently, spine-related pain is diagnosed comprehensively based on objective and subjective findings by each physician based on their experience.

Imaging diagnosis is an objective finding-based judgement made by physicians. For spinal disease, bone deformation, loss of the intervertebral space, presence of nonstandard movement, and disturbance of bone arrangement can be observed on radiology and computed tomography (CT). On magnetic resonance imaging (MRI), the relationship between the nerve system and surrounding structures and water component abnormalities, such as hemorrhage and tissue edema, can be closely observed. In elderly patients, degeneration is observed at multiple sites in many cases regardless of clinical symptoms, and identification of the responsible lesion is necessary. Previously, many physicians regarded neurological clinical findings as objective findings with the highest priority, while shape changes on MRI and CT as reference findings, and physicians who made accurate diagnoses through this procedure achieved favorable surgical outcomes[18,19]. Based on this situation, the priority of the current imaging findings is low as a material for making a judgment in the diagnostic process by spinal surgeons.

Surgical medical devices of the optical system have markedly advanced, endoscopy has rapidly spread, and spinal surgery is no exception[14-17]. As endoscopy enabled minimization of tissue invasion via the route of approach, improvement of diagnostic ability has become a proposition of improving surgical outcomes. New imaging diagnoses serving as a qualitative material for judgment, which are not possible by conventional imaging diagnosis that detects only changes in the shape, are expected.

Computer-aided engineering (CAE) has helped to reduce trial manufacturing costs and shorten the trial manufacturing period in the industrial field since 1970[1]. In CAE, load generation was simulated at the design stage using a specific Poisson's ratio and Young's modulus of each

hard material, thereby enabling visualization and quantification of the structure at fragile sites. CAE succeeded in visualizing and quantifying diagnostic values other than the shape through fusing contact, constraint, and loading conditions with the characteristic value of the material, which became the new judgement criteria.

The finite element method (FEM) has been utilized to analyze the developmental mechanism of the fracture of bone components, which are hard materials, and to judge the effects of fixation[2-10]. Additionally, preoperative investigation using a 3D printed model is now covered by the national health insurance[11,12]. Utilization of 3D reconstituted images for navigation based on CT DICOM data has also been progressing in the spinal surgery field[13]. However, no imaging diagnosis method capable of sufficiently expressing the effects of less invasive nerve root decompression, such as full endoscopic spinal surgery (FESS), has been developed. On MRI of patients with clinical improvement of nerve root symptoms after FESS, only findings of nerve root defects similar to those in the preoperative image are acquired in the current state.

We considered that by accurately setting Poisson's ratio and Young's modulus of soft materials, such as the ligament and intervertebral disc, the contact areas and contact pressures of the nerve root and dural sac can be evaluated by CAE and FEM. As CAE and FEM may be capable of visualizing and quantifying the preoperative diagnosis, preoperative simulation, and postoperative evaluation of surgical procedures useful for less invasive pin-point decompression, such as FESS, we evaluated them in this study.

2. Methods

2.1. Lumbar case presentation

A 67-year-old woman was referred to our department for sharp radiating pain in the anterior surface of the thigh due to L3 vertebral fracture-associated left L3 radiculopathy. As her pain developed during standing up and sitting motions, she had been bedridden for 3 months before the first examination and had difficultly moving even in a wheelchair. She had rheumatism treatment-induced secondary osteoporosis and pulmonary fibrosis, and was mainly based on the respiratory function test findings. Our hospital anesthesiologist deemed prolonged general anesthesia accompanied by intubation to be inapplicable and requested us to plan less invasive surgery.

We planned percutaneous endoscopic interlaminar partial laminectomy for nerve root decompression applicable under sedative local anesthesia[14-17], and additionally planned to extend the bilaterally laminectomy.

The patient sat for 2 hours postoperatively, and no radiating pain was observed in the left thigh. The following morning, the patient was able to walk for 5 m without pain while holding on to something. The chief clinical symptoms were resolved by percutaneous endoscopic foraminotomy and partial laminectomy. The patient underwent rehabilitation and achieved the goal of 5-m indoor movement at 6 months postoperatively, but outdoor movement required wheelchair use and her condition was the same as that before having the fracture. Pain did not recur throughout the 6-month postoperative period. The patient's satisfaction level with the surgery and referring physician was high at 6 months postoperatively[18-19].

Bone cutting of the planned range was confirmed on CT myelography. On MRI myelography, no change after surgery was noted, and the deficit of the dural canal and nerve root in the fracture region remained defective. No progression of deformation or new fracture was noted on radiology.

2.2 Cervical case presentation

A 61-year-old woman was referred to our department for sharp radiating pain in the left neck, back, and forearm due to C5-6 herniated disc associated with left C6 radiculopathy. She developed pain during the chin up motion for drinking. She had been receiving medication therapy and block injection for 3 months before the first our examination. She had difficulty working in medical education offices without many medications. She had requested less invasive surgery for her short hospital stay.

We planned percutaneous endoscopic foraminotomy for C6 nerve root decompression[14-17]. The patient sat for 2 hours postoperatively, and no radiating pain was reproduced around the left shoulder and forearm. Her hospital stay was 3 days long as she wished, and had no pain in the wound. The chief clinical symptoms were resolved by percutaneous endoscopic foraminotomy. She had left thumb numbness, but her pain during chin up motion did not recur throughout the 6-month postoperative period. Patient satisfaction with the surgery and referring physician was high at 6 months postoperatively[18-19].

Bone cutting of the planned range was confirmed on CT. On MRI myelography, no change after surgery was noted, and the deficit of the dural canal and nerve root in the region remained defective. No progression of deformation was noted on radiology.

2.3 FEM

First, we selected Mechanical Finder® of the Research Center of Computational Mechanics, Inc. as the analytical tool because of its ability to evaluate a spondylosis case using FEM. We investigated whether it is possible to reproduce loading in a lumbar standing position and a cervical extension position, visualize reductions in the contact area and contact pressure as color changes, and quantify the area and pressure postoperatively by FEM regarding the effects of nerve root decompression by percutaneous endoscopic foraminotomy, which cannot be expressed by conventional MRI.

The 3D model was reconstructed individually based on the DICOM data of two examinations, CT after preoperative myelography, and after surgery(Fig.1). The images were acquired using Toshiba Aquillion64 at a 0.5-mm slice width.

This study was not supported by any research funding. The study was approved by the Institutional Review Board (No. 191126-2) and we have undertaken and that it conforms to the provisions of the Declaration of Helsinki in 1995 (as revised in Brazil 2013). Informed consent was obtained by all participants in this study.

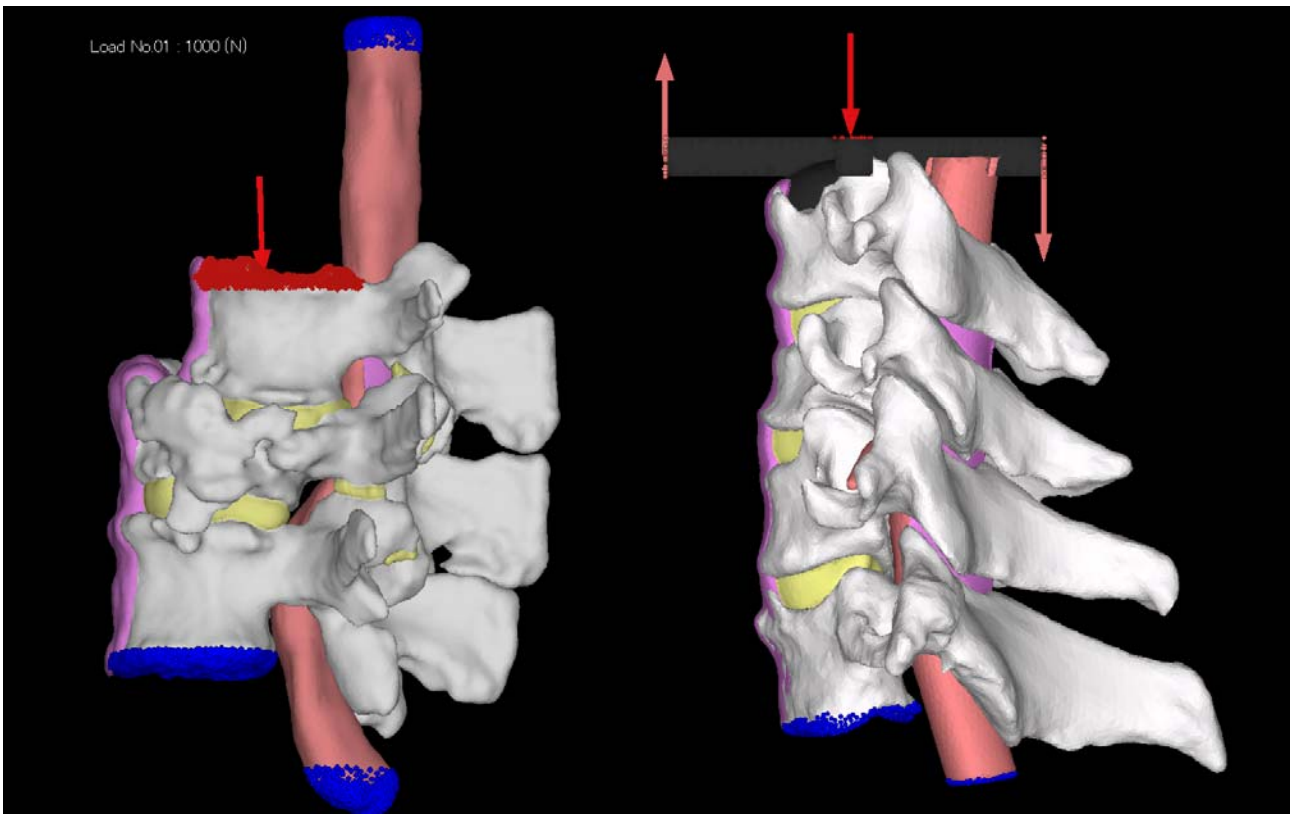

Fig. 1: Analytical lumbar and cervical model. Left: A 3D model of the L2-4 vertebrae, intervertebral discs, and dural canal reconstructed from CT data. For the load, 1,000 N was loaded in the gravity direction on the cranial-side end plate of L2. Right: A 3D model of the C4-7 vertebrae, intervertebral discs reconstructed from CT data and the dural sac from MR myelography data. 3.0 degree was loaded in extension on the disc of C5-6.

2.4 Lumbar model

The modeled range was the 2nd to 4th lumbar vertebrae, near the dural canal, intervertebral discs, yellow ligament, facet joint cartilage, and anterior longitudinal ligament as 3-dimensional elements and the intertransverse, supraspinous, and interspinous ligaments as trust elements (Fig. 1 left). The dural canal and intervertebral discs were handled as homogenous inner structures and quantified (Table 1). Regarding model limitations, as analysis setting the initial pressure in the dural canal cannot be performed, the initial pressure was handled as absent.

The loading and constraint conditions were set based on the assumption of the load in the standing position. The inferior surface of the 4th lumbar vertebra was constrained, and 1,000 N was vertically loaded on the superior surface of the 2nd lumbar vertebra. The upper and lower ends of the dural canal in the model range were constrained. The characteristics of the bone and soft tissue materials were specified as shown in Tables 1. The contact was set as follows: the dural canal contacted the posterior vertebral surfaces of the 2nd to 4th lumbar vertebrae, intervertebral discs, yellow ligament, and intervertebral joints preoperatively, and the contact between the bone cutting region and left yellow ligament disappeared postoperatively. The total contact areas and changes in the maximum contact pressure preoperatively and postoperatively were analyzed.

Table 1. Material constants of the components of the analytical model

Materials	**Young's modulus (MPa)**	**Poisson's ratio**	**References**
Vertebrae	ρ=0.0 E=0.001 0<ρ＜0.27 E=33900ρ^2.20 0.27＜ρ＜0.6 E=5307ρ＋469 0.6≦ρ E=10200ρ^2.01	0.4	[16]
Disc	4.20	0.45	[2,18]
Ligamentum flavum	15.0	0.3	[2,18]
Facet joint	20.0	20.0	[18]
Anterior longitudinal ligament	15.0	0.3	[2,18]
Dural sac	2.93	0.44	[10,18]
Nerve root	1.19	0.44	[10,18]
Materials	**Strain range: ε**	**Tension: T (N)**	**References**
Transverse ligament	ε＜0.0 0≦ε＜0.18 0.18≦ε	T=0.0 T=17.78ε T=105.73ε-15.83	[18]
Interspinous ligament	ε＜0.0 0≦ε＜0.14 0.14≦ε	T=0.0 T=400.00ε T=464.00ε-8.96	[18]

Supraspinous ligament	$\varepsilon < 0.0$	$T=0.0$	
	$0 \leqq \varepsilon < 0.20$	$T=240.0\varepsilon$	[18]
	$0.20 \leqq \varepsilon$	$T=450.0\varepsilon-42.0$	

2.5 Cervical model

The modeled range was the 4th to 7th cervical vertebrae, nearby dural canal, intervertebral discs, yellow ligament, facet joint cartilage, and anterior longitudinal ligament as 3-dimensional elements(Fig. 1 right). The dural canal and intervertebral discs were handled as homogenous inner structures and quantified. Regarding model limitations, as analysis setting the initial pressure in the dural canal cannot be performed, the initial pressure was handled as absent.

The loading and constraint conditions were set based on the assumption of the load in the extension position. The inferior surface of the 7th cervical vertebra was constrained, and 3.0° was loaded on the 5th to 6th disc. The lower ends of the dural canal in the model range were constrained. The characteristics of the bone and soft tissue materials are listed in Tables 1. The contact was set as follows: the dural canal contacted the posterior vertebral surfaces of the 4th to 7th cervical vertebrae, intervertebral discs, yellow ligament, and intervertebral joints preoperatively, and the contact between the bone cutting region and left yellow ligament disappeared postoperatively. The total contact areas and changes in the maximum contact pressure preoperatively and postoperatively were analyzed.

3. Results

3.1 Lumbar case

The contact area between the dural canal and other regions decreased from 62.7 to 12.7 mm^2 (-79.7%, Fig. 2), and the pressure decreased from 1.90 to 0.58 MPa.(-69.5%) The position loaded with the maximum contact pressure was near the medial cranial end of the left L3 superior articular process preoperatively, and it moved to a site near the cranial end of the L4 spinous process slightly to the right of the midline after surgery. Regarding the equivalent stress on the dural canal, approximately 0.2 MPa from the posterior side was observed on the left L3 nerve root bifurcation preoperatively, but it disappeared postoperatively.

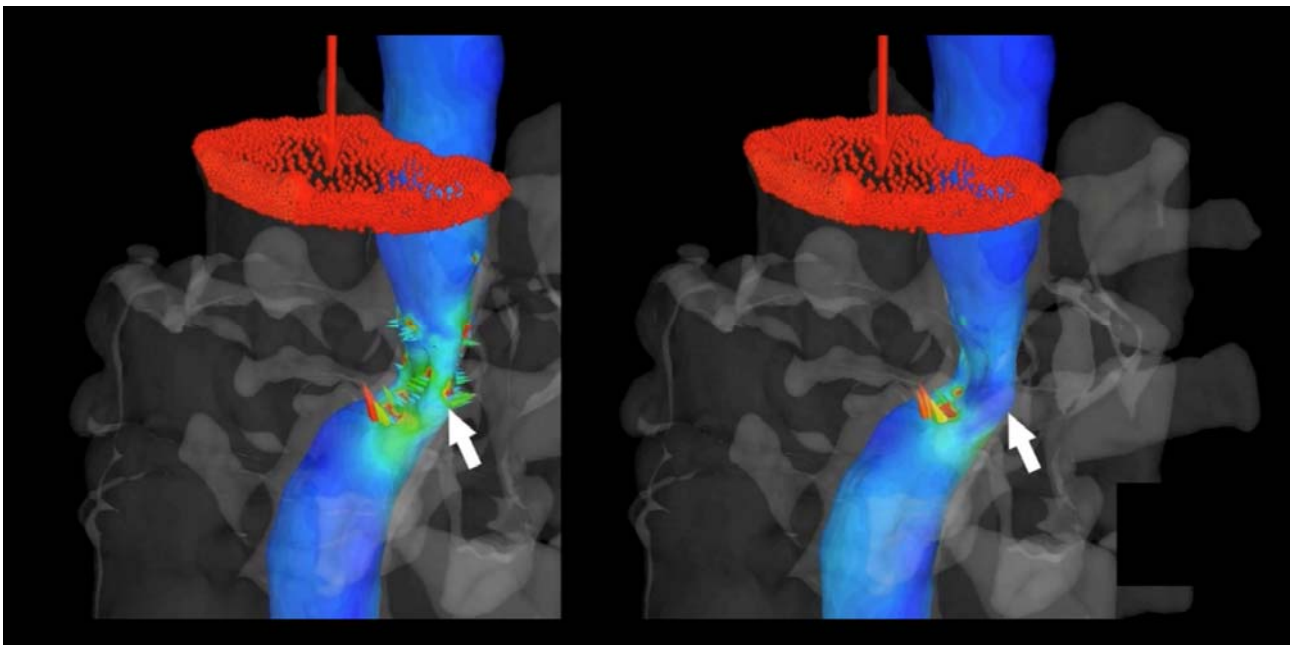

Fig. 2: Equivalent stress on the dural canal. The white arrow indicates the left L3 nerve root bifurcation. The left : before and right: after surgery. Before surgery, 0.2-MPa stress was disappeared after surgery.

3.2 Cervical case

The contact area between the dural canal and other regions decreased from 0.50 to 0.35 mm^2 (-30.0%, Fig. 3), and the pressure decreased from 0.15 to 0.10 MPa (-33.3%). Regarding the equivalent stress on the dural canal, approximately 0.2 MPa from the posterior side was observed on the left C6 nerve root proximal foramen preoperatively, but it disappeared postoperatively.

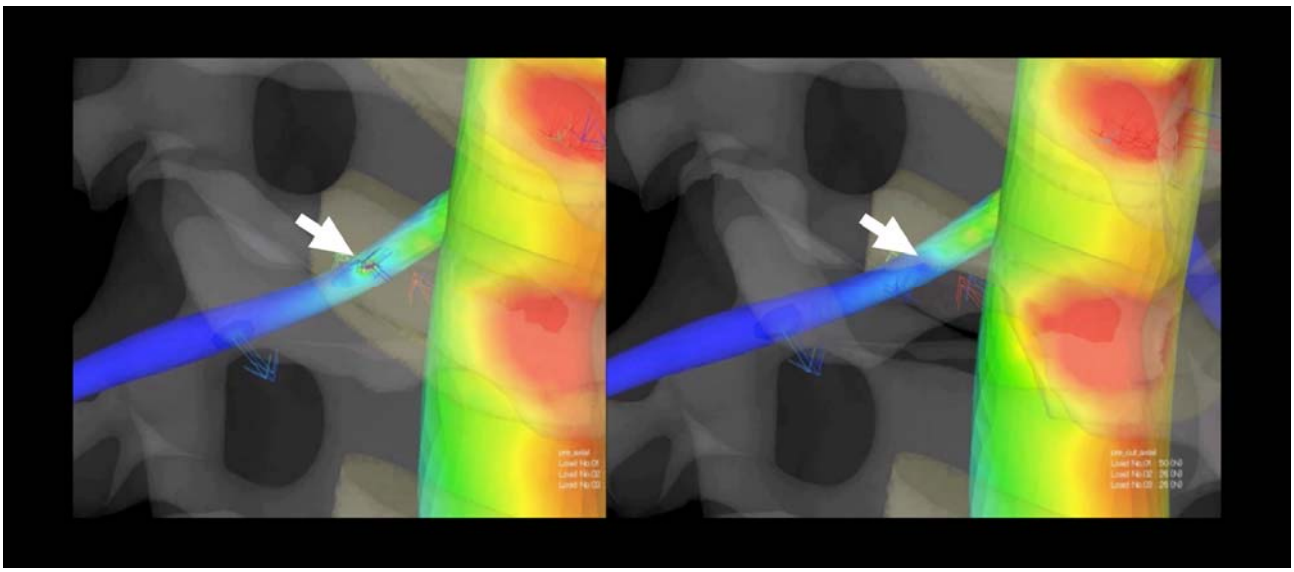

Fig. 3: Equivalent stress on the dural canal. The white arrow indicates the left C6 nerve root. The left : before and right: after surgery. Before surgery, 0.2-MPa stress was disappeared after surgery.

4. Discussion

4.1 Value of FEM as an evaluation method of less invasive surgery

There were three characteristics of less invasive surgery in the present lumbar patient. First, the clinical symptoms were different from the imaging findings. Second, the surgery had a time constraint due to the anesthesia method and nerve root decompression because of the minimum necessary bone cutting region required. Third, the effects of decompression were not confirmed by conventional postoperative imaging evaluation alone. These problems are frequently noted in less invasive spinal surgery.

4.2 Value of FEM for preoperative diagnosis

The clinical diagnosis of this patient was left L3 radiculopathy, and imaging diagnosis was right side-dominant L2-3 spinal canal and foraminal stenosis. Radiology, MRI, myelography, nerve root puncture, and CT myelography were performed. The bases for the definite preoperative diagnosis of left L3 radiculopathy were the clinical diagnosis and pain reproduced during left L3 nerve root block therapy. The bases for performing left L3 nerve root block were clinical symptoms and stenosis noted at the L2-3 intervertebral disc level in the axial view on MRI. The reason for the absence of complaints on the right side despite severe stenosis being noted on the right side was unclear[20-22] but we suspect the unstable state had occurred root irritation at the left pedicle fractured portion. We must often decide whether to take priority in clinical data or imaging findings since the spread of less invasive surgery for pain.

The finding of preoperative equivalent stress on the dural canal investigated by FEM was the presence of approximately 0.2-MPa stress from the posterior side at the L2-3 disc level only on the left side. On the right side, approximately 0.1-MPa stress from the side of the anterior dural canal was present, but almost no stress from the posterior side was loaded (Fig. 2).

If the neurological and conventional imaging findings were combined with the FEM findings, the preoperative diagnosis may have been left L3 radiculopathy. As FEM presents not only the shape, but also stresses loaded on the nerve root and dural canal as colors, location, and values based on CT data, it provides a new tool for diagnosis. Difficult cases with deviation between the clinical symptoms and imaging diagnosis may be reduced by FEM. FEM may serve as a judgement criterion to effectively identify the responsible lesions.

4.3 Value of FEM for preoperative simulation

For the present lumbar patient, surgery was planned based primarily the clinical diagnosis. Our strategy was to add laminectomy targeting dilatation of the spinal canal if time permitted after left L3 nerve root decompression. Indeed, we performed left L3 nerve root decompression within 80 minutes and bilateral L3 laminectomy and partial excision of the yellow ligament in an additional 100 minutes; the patient's symptoms disappeared after surgery.

Next, we discuss the changes that would have been made to the surgical strategy in this case if preoperative simulation had been performed by FEM. Surgery for left L3 nerve root decompression would have been divided into three procedures: foraminotomy, L3 laminectomy, and excision of yellow ligament, and difference in the effects of foraminotomy alone, foraminotomy and L3 laminectomy, and all three procedures would have been investigated. Then, the effects of L3 laminectomy, including setting the range of laminectomy to the side alone and the bilateral sides, would have been investigated. Changes in the equivalent stress on the dural canal would have been observed to confirm the minimum extent necessary during surgery.

If data of the equivalent stress on the dural canal from the posterior side were acquired before surgery, we would have completed surgery with left L3 nerve root decompression alone within 80 minutes. Additionally, if foraminotomy simulation was performed in detail at 1-mm units to investigate how small we could cut the bone, it would have been possible to complete surgery within 60 minutes and improve the clinical symptoms.

The cervical case's most stressed area was proximal point where we suspected. We had believed distal foraminal area was responsible region from axial and sagittal MRI images. If we had known this FEM simulation report before surgery, we planned additional margin to decompress for proximal responsible C5 lamina area.

4.4 Value of FEM for postoperative evaluation

When nerve root decompression was applied in the minimum bone cutting range by FESS, the surgery was unable to be sufficiently justified by conventional evaluation by imaging. The bone cutting region can be intuitively identified by comparison of the reconstituted 3D CT image before and after surgery, but skills are necessary to understand it with conventional sagittal, coronal, and axial CT bone data.

MRI was performed postoperatively, but no change from the preoperative findings was noted in the dural canal defect at the L2 to L3 disc level on MR myelography. Although the objective was achieved clinically, it did not serve as a material justifying the surgery because of the absence of a change in the image. We have experienced this in many cases since we initiated FESS and felt the necessity of developing a new evaluation method that intuitively expresses the effect.

We consider the postoperative improvement of symptoms after FESS to be insufficient. There are too many causes, such as disorientation readily occurring due to the small surgical field, inefficient time usage because the bone cutting tool is limited to those with a speed of 20,000 rpm or lower and a diameter of ≤3.5 mm, and the clinical symptoms and imaging findings are different in many patients. When the effects were insufficient, the case was reevaluated, but there was a limit in evaluation by the conventional method because it is difficult to identify the lesion responsible by investigating only shape changes, including defective shadows of the dural canal and nerve root alone in many patients indicated for FESS.

In this study, we expressed the effects of nerve root decompression by the color, location, and values, and acquired findings corresponding to improvement of the clinical symptoms. FEM visualizes and quantifies the effects of FESS, and succeeds in justification, which could not be performed by the conventional method. We considered FEM to function as a postoperative evaluation method of surgery after FESS, and it is capable of accurately presenting the following strategy even when decompression is insufficient.

4.5 Study Limitations

For FEM analysis, Poisson's ratio and Young's modulus of each structure component are necessary (Table 1). In this analysis, the values used in preceding studies were cited[2-10]. The subjects of the preceding studies were the femur and scoliosis in middle-aged men. Analysis based on Poisson's ratio and Young's modulus measured in the lumbar vertebra would have been ideal for the present patient, and basic experiments using human degenerated lumbar vertebrae and measurements during surgery increase the accuracy of FEM of degenerative disease of the lumbar spine in the future. However, regarding the detection of changes postoperatively, we considered that if relative changes can be expressed, surgical effects can be expressed and values remain as references, being sufficient as an experimental system.

This analysis was performed for loading only in vertical postures such as sitting, standing and extension positions. By analyzing these in rotation, lateral bending, and anteroposterior flexion, further improvement of the treatment outcome can be expected. However, experts required 2 months to analyze one postural condition plus the corresponding costs for the analysis. Owing to the limited research budget, only the lumbar vertical postures and the cervical extension posture were analyzed. When the content of this analysis is generalized and the analysis can be performed within a short time acceptable for clinical sites at a medical economically acceptable cost, analysis may be easily performed under many specified conditions and widely accepted by spinal surgeons.

4.6 Future study prospects

Preoperative simulation employing a 3D printed model is now covered by the National Health insurance[11-12]. Preoperative diagnosis, surgical plan preparation, and postoperative evaluation by computer-aided engineering(CAE) or FEM may be applied for coverage by national health insurance if software resolving problems that are time- and cost-efficient is developed. Analysis was performed on the lumbar and cervical spines. We plan to analyze the effects of FESS in the thoracic spine by FEM in the next study. Additionally, to improve the accuracy, accumulation of measured data of Poisson's ratio and Young's modulus of the above-mentioned spine components cannot be avoided. Lastly, we plan to investigate the possibility of visualization and quantification of spine-related pain by statistical analysis of neurological findings, subjective pain symptoms, and CAE or FEM data.

We succeeded in visualizing and quantifying the effects of nerve root decompression by FESS in the lumbar and the cervical vertebrae using FEM. In the present patient, the contact area and pressure of the nerve tissue decreased to 30%-80% and 33%-67%, respectively, postoperatively, and their radiculopathy was relieved. FEM may has been develop as a new imaging diagnostic methods useful for making a preoperative diagnosis, surgical simulation, and postoperative evaluation required in less invasive spinal surgery such as FESS. FEM allows the simulation of the dynamic standing or extension position condition.

Acknowledgement:

The authors declare that there are no conflicts of interest and source of funding. Authors' contributions Yoshihiro Kitahama designed the study and wrote the initial draft of the manuscript. Katsuhiko Sakai and Hiroo Shizuka contributed to analysis and interpretation of data and assisted in the preparation of the manuscript. All other authors have contributed to data collection and interpretation, and critically reviewed the manuscript. All authors approved the final version of the manuscript and agree to be accountable for all aspects of the work in ensuring that questions related to the accuracy or integrity of any part of the work are appropriately investigated and resolved.

References

1. Chryssolouris G, Mavrikios D, Papakostas N, D Mourtzis, G Michalos, K Georgoulias. Digital manufacturing: history, perspectives, and outlook. P I Mech Eng B-J Eng Manuf 2009;223(5):451–462. doi:10.1243/09544054JEM1241

2. Chen CS, Cheng CK, Liu CL, Lo WH. Stress analysis of the disc adjacent to interbody fusion in lumbar spine. Med Eng Phys. 2001;23(7):483 -491. doi:10.1016/s1350-4533(01)00076-5

3. Imai K, Ohnishi I, Yamamoto S, Nakamura K. In vivo assessment of lumbar vertebral strength in elderly women using computed tomography-based nonlinear finite element model. Spine (Phila Pa 1976). 2008;33(1):27 -32. doi:10.1097/BRS.0b013e31815e3993

4. Keyak JH, Rossi SA, Jones KA, Skinner HB. Prediction of femoral fracture load using automated finite element modeling. J Biomech. 1998;31(2):125 -133. doi:10.1016/s0021-9290(97)00123-1

5. Keyak JH, Lee IY, Skinner HB. Correlations between orthogonal mechanical properties and density of trabecular bone: use of different densitometric measures. J Biomed Mater Res. 1994;28(11):1329 -1336. doi:10.1002/jbm.820281111

6. Keyak JH, Rossi SA. Prediction of femoral fracture load using finite element models: an examination of stress- and strain-based failure theories. J Biomech. 2000;33(2):209 -214. doi:10.1016/s0021-9290(99)00152-9

7. Kim HJ, Chun HJ, Kang KT, Lee HM, Kim HS, Moon ES, Park JO, Hwang BH, Son JH, Moon SH. A validated finite element analysis of nerve root stress in degenerative lumbar scoliosis. Med Biol Eng Comput. 2009;47(6):599 -605. doi:10.1007/s11517-009-0463-y

8. Murase K, Morita F, Yoshino N, Fukuda Y, Tsutsumi S, Ikeuchi K. Impact load transmission of human knee joint using in vitro drop-tower test and three-dimensional finite element simulation. J Biomech Sci Eng 2007;2(4):218-227. doi: 10.1299/jbse.2.218

9. Singh A, Lu Y, Chen C, Cavanaugh JM. Mechanical properties of spinal nerve roots subjected to tension at different strain rates. J Biomech. 2006;39(9):1669 -1676. doi:10.1016/j.jbiomech.2005.04.023

10. Sagnac E, Arnoux PJ, Garo A, Aubin CE. Finite element analysis of the influence of loading rate on a model of the full lumbar spine under dynamic loading conditions. Med Biol Eng Comput. 2012;50(9):903 -915. doi:10.1007/s11517-012-0908-6

11. Martelli N, Serrano C, van den Brink H, Pineau J, Prognon P, Borget I , Batti SE. Advantages and disadvantages of 3-dimensional printing in surgery: A systematic review. Surgery. 2016;159(6):1485 -1500. doi:10.1016/j.surg.2015.12.017

12. Mizutani J, Matsubara T, Fukuoka M, Tanaka N, Iguchi H, Furuya A, Okamoto H, Wada I, Otsuka T. Application of full-scale three-dimensional models in patients with rheumatoid cervical spine. Eur Spine J. 2008;17(5):644 -649. doi:10.1007/s00586-008-0611-3

13. Furukawa J, Miyake H, Tanaka K, Sugimoto M, Fujisawa M. Console-integrated real-time three-dimensional image overlay navigation for robot-assisted partial nephrectomy with selective arterial clamping: early single-centre experience with 17 cases. Int J Med Robot. 2014;10(4):385 -390. doi:10.1002/rcs.1574

14. Kitahama Y, Matsui G, Minami M, Kawaoka T, Otome K, Nakamura M. Posterolateral percutaneous endoscopic discectomy with free-running electromyography monitoring under general anesthesia. Mini-invasive Surg 2017;1(9):109-114. doi:10.20517/2574-1225.2017.11

15. Ruetten S, Komp M, Merk H, Godolias G. Full-endoscopic interlaminar and transforaminal lumbar discectomy versus conventional microsurgical technique: a prospective, randomized, controlled study. Spine (Phila Pa 1976). 2008;33(9):931 -939. doi:10.1097/BRS.0b013e31816c8af7

16. Sairyo K, Chikawa T, Nagamachi A. State-of-the-art transforaminal percutaneous endoscopic lumbar surgery under local anesthesia: Discectomy, foraminoplasty, and ventral facetectomy. J Orthop Sci. 2018;23(2):229 -236. doi:10.1016/j.jos.2017.10.015

17. Yeung AT, Yeung CA. Minimally invasive techniques for the management of lumbar disc herniation. Orthop Clin North Am. 2007;38(3):363 -vi. doi:10.1016/j.ocl.2007.04.005

18. Atlas SJ, Keller RB, Wu YA, Deyo RA, Singer DE. Long-term outcomes of surgical and nonsurgical management of sciatica secondary to a lumbar disc herniation: 10 year results from the maine lumbar spine study. Spine (Phila Pa 1976). 2005;30(8):927 -935.

doi:10.1097/01.brs.0000158954.68522.2a

19. Weinstein JN, Tosteson TD, Lurie JD, Tosteson A, Blood E, Herkowitz H, Cammisa F, Albert T, Boden SD, Hilibrand A, Goldberg H, Berven S, An H. Surgical versus nonoperative treatment for lumbar spinal stenosis four-year results of the Spine Patient Outcomes Research Trial. Spine (Phila Pa 1976). 2010;35(14):1329 -1338. doi:10.1097/BRS.0b013e3181e0f04d

20. Byun WM, Ahn SH, Ahn MW. Value of 3D MR lumbosacral radiculography in the diagnosis of symptomatic chemical radiculitis. AJNR Am J Neuroradiol. 2012;33(3):529 -534. doi:10.3174/ajnr.A2813

21. Cesaro P, Mann MW, Moretti JL,G Defer, B Roualdés, J P Nguyen, J D Degos. Central pain and thalamic hyperactivity: a single photon emission computerized tomographic study. Pain. 1991;47(3):329 -336. doi:10.1016/0304-3959(91)90224-l

22. Morton DL, Sandhu JS, Jones AK. Brain imaging of pain: state of the art. J Pain Res. 2016;9:613 -624. Published 2016 Sep 8. doi:10.2147/JPR.S60433